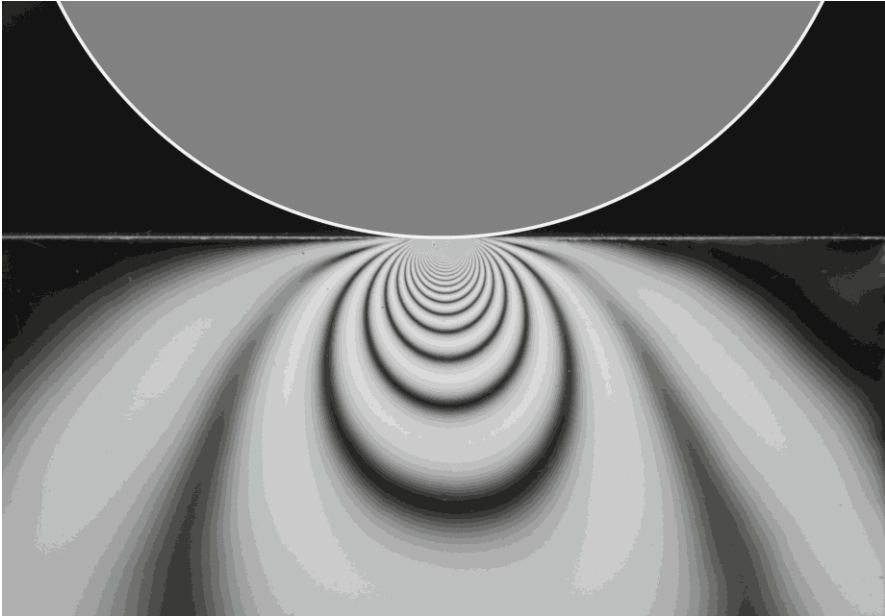


5 Rigorous Treatment of Contact Problems – Hertzian Contact



In this chapter, a method is illustrated to find the exact solutions of contact problems in the framework of the “half-space approximation.” We examine, in detail, the classical contact problem of normal contact between a rigid sphere and an elastic half-space, which is often used to analyze more complex models.

As a preparatory step, we will summarize a few results of the theory of elasticity that have a direct application to contact mechanics. We consider the deformations in an elastic half-space, which are caused by a given stress acting upon its surface. The calculation of the deformation of an elastic body whose surface is being acted upon by a force (“direct problem of the theory of elasticity”) is much easier than the solution of contact problems, because in the latter, neither the stress distribution, nor the contact area are known to begin with. The classic solutions from Hertz (non-adhesive contact) and Johnson, Kendall, and Roberts (adhesive contact) use the known solutions for “direct problems” as building blocks to the construction of a solution for a contact problem.

5.1 Deformation of an Elastic Half-Space being Acted upon by Surface Forces

We consider an elastic medium that fills an infinitely large half-space (i.e. its only boundary is an infinite plane). Under the influence of the forces that act on the free surface, the medium is deformed. We place the xy -plane on the free surface of the medium; the filled area corresponds to the positive z -direction. The deformations in the complete half-space can be defined in analytical form and found in textbooks over the theory of elasticity¹. Here, we will only mention the formula for the displacement from a force acting at the origin in the positive z -direction.

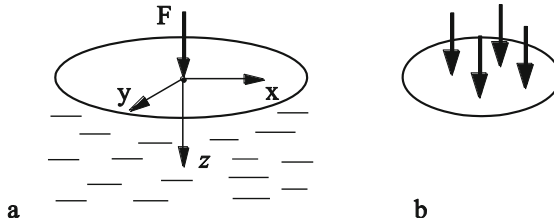


Fig. 5.1 (a) A force acting on an elastic half-space; (b) a system of forces acting on a surface.

The displacement caused by this force is calculated using the following equations:

$$u_x = \frac{1+\nu}{2\pi E} \left[\frac{xz}{r^3} - \frac{(1-2\nu)x}{r(r+z)} \right] F_z, \quad (5.1)$$

$$u_y = \frac{1+\nu}{2\pi E} \left[\frac{yz}{r^3} - \frac{(1-2\nu)y}{r(r+z)} \right] F_z, \quad (5.2)$$

$$u_z = \frac{1+\nu}{2\pi E} \left[\frac{2(1-\nu)}{r} + \frac{z^2}{r^3} \right] F_z, \quad (5.3)$$

with $r = \sqrt{x^2 + y^2 + z^2}$.

In particular, one obtains the following displacements of the free surface, which we have defined as $z = 0$:

$$u_x = -\frac{(1+\nu)(1-2\nu)}{2\pi E} \frac{x}{r^2} F_z, \quad (5.4)$$

¹ L.D. Landau, E.M. Lifschitz, Theory of elasticity. (Theoretical Physics, Vol. 7), 3rd edition, 1999, Butterworth-Heinemann, Oxford, §§ 8,9.

$$u_y = -\frac{(1+\nu)(1-2\nu)}{2\pi E} \frac{y}{r^2} F_z, \quad (5.5)$$

$$u_z = \frac{(1-\nu^2)}{\pi E} \frac{1}{r} F_z, \quad (5.6)$$

with $r = \sqrt{x^2 + y^2}$.

If several forces act simultaneously (Fig. 5.1 b), we will get a displacement as the sum of the respective solutions that result from every individual force.

We will continue to work in approximation of the half-space, in which it is assumed that the gradient of the surfaces in the area of contact and within relative proximity is much smaller than one, so that in a first order approximation, the surfaces are “even.” Although the contact constraints for the two surfaces must continue to be met, the relation between the surface forces and the displacements can be seen, however, exactly as they appear with an elastic half-space.

For contact problems *without friction*, only the z -component of the displacement (5.6) is of interest within the framework of the half-space approximation. Especially in the case of a continuous distribution of the normal pressure $p(x, y)$, the displacement of the surface is calculated using

$$u_z = \frac{1}{\pi E^*} \iint p(x', y') \frac{dx' dy'}{r}, \quad r = \sqrt{(x-x')^2 + (y-y')^2} \quad (5.7)$$

with

$$E^* = \frac{E}{(1-\nu^2)}. \quad (5.8)$$

Before we move on to actual contact problems, we want to solve two preparatory problems. We assume that a pressure with a distribution of $p = p_0 \left(1 - r^2 / a^2\right)^n$ is exerted on a circle-shaped area with the radius a and search for the vertical displacement of the surface points within the area being acted upon by the pressure.

a. Homogeneous Normal Displacement ($n = -1/2$).

The coordinate system used is shown in Fig. 5.1. The normal stress is distributed according to the equation

$$p = p_0 \left(1 - \frac{r^2}{a^2}\right)^{-1/2}. \quad (5.9)$$

The resulting vertical displacement is²:

$$u_z = \frac{\pi p_0 a}{E^*}, \quad r \leq a. \quad (5.10)$$

The vertical displacement is the same for all points in the contact area. From this result, it directly follows how we can produce the assumed pressure distribution: it is produced by the indentation of a rigid cylindrical rod into an elastic half-space. The total force acting on the area under pressure is equal to

$$F = \int_0^a p(r) 2\pi r dr = 2\pi p_0 a^2. \quad (5.11)$$

The stiffness of the contact is defined as the relationship between the force F and the displacement u_z :

$$k = 2aE^*. \quad (5.12)$$

If written in the form³

$$k = 2E^* \beta \sqrt{\frac{A}{\pi}}, \quad (5.13)$$

where A is the contact area of the rigid indenter, Equation (5.12) is also valid for cross-sections that are not round. The constant β always has an order of magnitude of 1:

Round cross-section:	$\beta=1.000$	
Triangular cross-section:	$\beta=1.061$	(5.14)
Rectangular cross-section:	$\beta=1.021$	

b. Hertzian Pressure Distribution ($n = 1/2$).

For the pressure distribution of the form

$$p = p_0 \left(1 - \frac{r^2}{a^2}\right)^{1/2}, \quad (5.15)$$

the resulting vertical displacement (Appendix A) is

$$u_z = \frac{\pi p_0}{4E^* a} (2a^2 - r^2), \quad r \leq a. \quad (5.16)$$

The total force follows as

² A detailed derivation can be found in Appendix A.

³ Q. Li, V.L. Popov, Indentation of flat-ended and tapered indenters with polygonal geometries, *Facta Universitatis, series: Mechanical Engineering*, 2016, v. 14, N. 3, pp. 241-249.

$$F = \int_0^a p(r)2\pi r dr = \frac{2}{3} p_0 \pi a^2 . \quad (5.17)$$

The displacement of the surface inside and outside of the area under pressure is shown in Fig. 5.2.

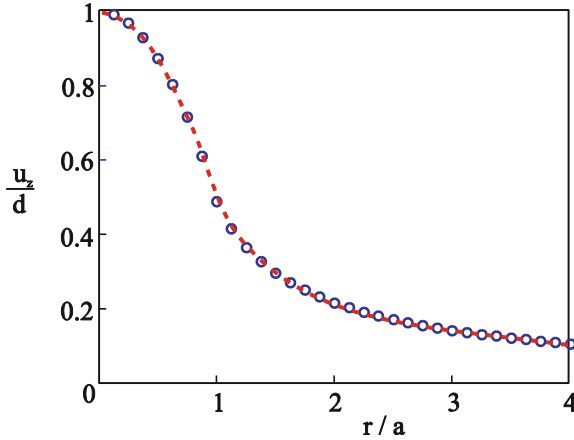


Fig. 5.2 Surface displacement u_z resulting from a pressure distribution (5.15); $d = u_z(0)$ is the indentation depth.

5.2 Hertzian Contact Theory

In Fig. 5.3, a contact between a rigid sphere and an elastic half-space is shown schematically. The displacement of the points on the surface in the contact area between an originally even surface and a rigid sphere of radius R is equal to

$$u_z = d - \frac{r^2}{2R} . \quad (5.18)$$

We have seen in (5.16) that a quadratic distribution of the vertical displacement results from a pressure distribution of the form in (5.15).

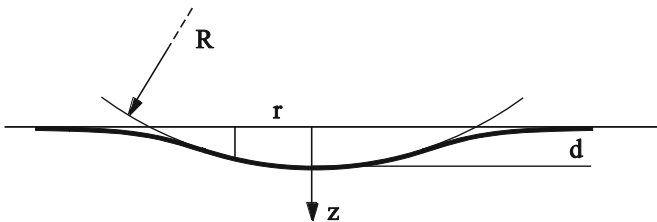


Fig. 5.3 A rigid sphere in contact with an elastic half-space.

We will try to find the parameters a and p_0 that cause exactly the displacement in (5.18):

$$\frac{1}{E^*} \frac{\pi p_0}{4a} (2a^2 - r^2) = d - \frac{r^2}{2R}. \quad (5.19)$$

The variables a and d must, therefore, fulfill the following requirements:

$$a = \frac{\pi p_0 R}{2E^*}, \quad d = \frac{\pi a p_0}{2E^*}. \quad (5.20)$$

It follows for the contact radius

$$a^2 = Rd \quad (5.21)$$

and for the maximum pressure

$$p_0 = \frac{2}{\pi} E^* \left(\frac{d}{R} \right)^{1/2}. \quad (5.22)$$

Substituting from (5.21) and (5.22) into (5.17) we obtain a normal force of

$$F = \frac{4}{3} E^* R^{1/2} d^{3/2}. \quad (5.23)$$

With (5.22) and (5.23), the pressure in the center of the contact area can be calculated as well as the contact radius as a function of the normal force:

$$p_0 = \left(\frac{6FE^{*2}}{\pi^3 R^2} \right)^{1/3}, \quad a = \left(\frac{3FR}{4E^*} \right)^{1/3}. \quad (5.24)$$

We can also determine the expression for the potential energy of the elastic deformation U . Since $-F = -\partial U / \partial d$, we obtain the following expression for U :

$$U = \frac{8}{15} E^* R^{1/2} d^{5/2}. \quad (5.25)$$

5.3 Contact between Two Elastic Bodies with Curved Surfaces

The results from Hertzian theory (5.21), (5.22), and (5.23) can also be used with few modifications in the following cases.

(A) If both bodies are elastic, then the following expression for E^* must be used:

$$\frac{1}{E^*} = \frac{1-\nu_1^2}{E_1} + \frac{1-\nu_2^2}{E_2}. \quad (5.26)$$

Here, E_1 and E_2 are the moduli of elasticity and ν_1 and ν_2 the Poisson's ratios of both bodies.

(B) If two spheres with the radii R_1 and R_2 are in contact (Fig. 5.4 a), then the equations (5.21), (5.22), and (5.23) are valid using the equivalent radius R :

$$\frac{1}{R} = \frac{1}{R_1} + \frac{1}{R_2}. \quad (5.27)$$

This is also valid if one of the radii is negative (Fig. 5.4 b). The radius of curvature is negative if the center of curvature lies outside of the medium.

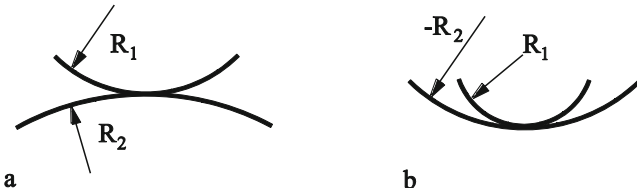


Fig. 5.4 Contact between two bodies with curved surfaces.

(C) In a contact between an elastic half-space and a rigid body with the principal radii of curvature of R_1 and R_2 (Fig. 5.5 a), an elliptical contact area results. The semi-axes are

$$a = \sqrt{R_1 d}, \quad b = \sqrt{R_2 d}. \quad (5.28)$$

Consequently, the contact area is calculated as⁴

$$A = \pi ab = \pi \tilde{R} d, \quad (5.29)$$

where the effective *Gaussian radius of curvature* of the surface is

$$\tilde{R} = \sqrt{R_1 R_2}. \quad (5.30)$$

This radius can also be used in place of R in other Hertzian relationships⁵.

⁴ Equations (5.28) represent only a rough estimation. On the other hand, equations (5.29) and (5.30) are valid with high accuracy as long as the ratio a/b is close to "1".

The pressure distribution is given by

$$p(x, y) = p_0 \sqrt{1 - \frac{x^2}{a^2} - \frac{y^2}{b^2}}. \quad (5.31)$$

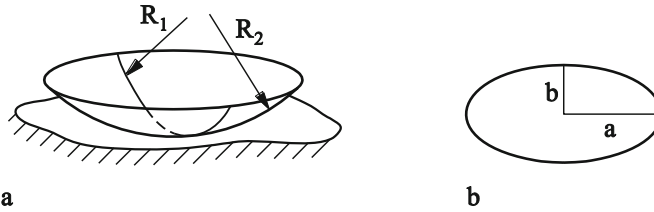


Fig. 5.5 A body with a curved surface (principal radii of curvature R_1 and R_2) in contact with an elastic half-space.

(D) If two elastic cylinders are in contact and lie on perpendicular axes with radii R_1 and R_2 (Fig. 5.6 a), then the distance between the surfaces of both bodies at the moment of the first contact (still without deformation) is given by

$$h(x, y) = \frac{x^2}{2R_1} + \frac{y^2}{2R_2}. \quad (5.32)$$

This is exactly in accordance with case (C) for ellipsoids with radii of curvature R_1 and R_2 . Therefore, Hertzian relations are valid, if the effective radius

$$\tilde{R} = \sqrt{R_1 R_2} \quad (5.33)$$

is used. If both cylinders have the same radii, $R = R_1 = R_2$, then the contact problem is equivalent to the contact problem between a sphere of radius R and an elastic half-space with an even surface.

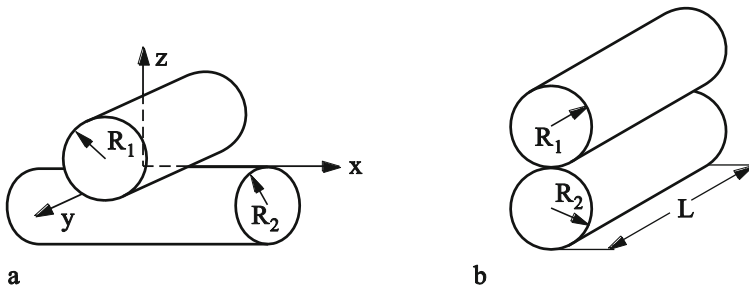


Fig. 5.6 (a) Two crossed cylinders in contact; (b) Two cylinders in contact with parallel axes.

⁵ This statement is not exact. The closer the ratio R_1 / R_2 is to 1, the more precise the Hertzian relationships hold. Even with a ratio of $R_1 / R_2 = 10$, however, Equation (5.23) can be applied to elliptical contacts with a precision of 2.5%.

(E) In the case of the contact between two cylinders with parallel axes (Fig. 5.6 b), the force is linearly proportional to the penetration depth (which we already saw in Chapter 2):

$$F \approx \frac{\pi}{4} E^* L d . \quad (5.34)$$

It should be noted here that the indentation depth in this so-called line contact is not unambiguously defined because of the logarithmic divergence of the displacement field at infinity. The exact definition of the indentation depth and the relation between the normal force and the indentation depth depends on the size and shape of the whole body. However, this dependence is weak (logarithmic) so that equation (5.34) can be used as a rough approximation. What is interesting is that the radius of curvature does not appear at all in the relationship (5.34). Half of the contact width is given through the equation

$$a \approx \sqrt{Rd} , \quad \frac{1}{R} = \frac{1}{R_1} + \frac{1}{R_2} , \quad (5.35)$$

as in the contact between two spheres and the pressure distribution is

$$p(x) = p_0 \sqrt{1 - \left(\frac{x}{a}\right)^2} . \quad (5.36)$$

The maximum pressure is equal to

$$p_0 = \frac{E^* d}{2 a} = \frac{E^*}{2} \left(\frac{d}{R}\right)^{1/2} = \left(\frac{E^* F}{LR}\right)^{1/2} . \quad (5.37)$$

5.4 Contact between a Rigid Cone-Shaped Indenter and an Elastic Half-Space

When indenting an elastic half-space with a rigid cone-shaped indenter (Fig. 5.7 a), the penetration depth and the contact radius are given through the relationship⁶

$$d = \frac{\pi}{2} a \tan \theta . \quad (5.38)$$

The pressure distribution has the form

⁶ Detailed derivation is seen in Problem 7 of this chapter.

$$p(r) = -\frac{Ed}{\pi a(1-\nu^2)} \ln \left(\frac{a}{r} + \sqrt{\left(\frac{a}{r}\right)^2 - 1} \right). \quad (5.39)$$

The stress has a logarithmic singularity (Fig. 5.7 b) at the point of the cone (at the center of the contact area). The total force is calculated as

$$F_N = \frac{2}{\pi} E^* \frac{d^2}{\tan \theta}. \quad (5.40)$$

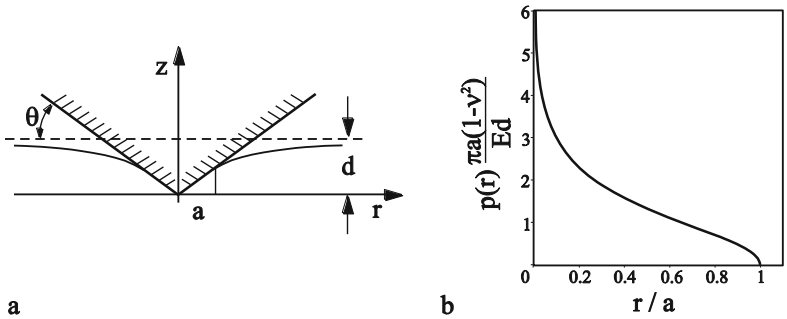


Fig. 5.7 (a) Contact between a rigid cone-shaped indenter and an elastic half-space; (b) Pressure distribution in the normal contact between a rigid cone-shaped indenter and an elastic half-space.

5.5 Internal Stresses in Hertzian Contacts

The stresses under the influence of a single, vertical force, F , acting at the origin, are defined by⁷

$$\sigma_{xx} = \frac{F}{2\pi} \left[-3 \frac{x^2 z}{r^5} + (1-2\nu) \left(\frac{x^2 (2r+z)}{r^3 (r+z)^2} - \frac{r^2 - rz - z^2}{r^3 (r+z)} \right) \right], \quad (5.41)$$

$$\sigma_{yy} = \frac{F}{2\pi} \left[-3 \frac{y^2 z}{r^5} + (1-2\nu) \left(\frac{y^2 (2r+z)}{r^3 (r+z)^2} - \frac{r^2 - rz - z^2}{r^3 (r+z)} \right) \right], \quad (5.42)$$

$$\sigma_{zz} = -\frac{3F}{2\pi} \frac{z^3}{r^5}, \quad (5.43)$$

⁷ H.G. Hahn, Elastizitätstheorie. Teubner, 1985.

$$\tau_{xy} = \frac{F}{2\pi} \left[-3 \frac{xyz}{r^5} + (1-2\nu) \frac{xy(2r+z)}{r^3(r+z)^2} \right], \quad (5.44)$$

$$\tau_{yz} = \frac{3F}{2\pi} \frac{yz^2}{r^5}, \quad (5.45)$$

$$\tau_{xz} = \frac{3F}{2\pi} \frac{xz^2}{r^5}. \quad (5.46)$$

The calculation of the stresses by an arbitrary normal pressure distribution p on the surface is made possible through superposition. The normal stress in the z -direction, σ_{zz} , is exemplary

$$\sigma_{zz}(x, y, z) = -\frac{3z^3}{2\pi} \iint_{(A)} \frac{p(x', y')}{\left((x-x')^2 + (y-y')^2 + z^2 \right)^{5/2}} dx' dy', \quad (5.47)$$

where $\iint_{(A)}$ means the integral over the area being acted upon by the pressure.

For the Hertzian pressure distribution in (5.15), various results are discussed in the following. Fig. 5.8 shows the stresses at the z -axis for $\nu=0.33$. All of the shear stresses are 0; for all points along the z -axis, the principal axes coincide with the coordinate axes. The analytical solution for the components of the stress tensors provides us with⁸

$$\sigma_{zz} = -p_0 \left(1 + \frac{z^2}{a^2} \right)^{-1}, \quad (5.48)$$

$$\sigma_{xx} = \sigma_{yy} = -p_0 \left[(1+\nu) \left(1 - \frac{z}{a} \arctan \frac{a}{z} \right) - \frac{1}{2} \left(1 + \frac{z^2}{a^2} \right)^{-1} \right]. \quad (5.49)$$

Furthermore, the maximum shear stress, $\tau_1 = \frac{1}{2} |\sigma_{zz} - \sigma_{xx}|$, is depicted in Fig. 5.8. One comes to the conclusion that the maximum shear stress lies in the interior, for $\nu=0.33$ at $z \approx 0.49a$. Fig. 5.9 shows the equivalent stress according to the von Mises criterion in the x - y plane:

$$\sigma_V = \frac{1}{\sqrt{2}} \left[(\sigma_{xx} - \sigma_{yy})^2 + (\sigma_{xx} - \sigma_{zz})^2 + (\sigma_{zz} - \sigma_{yy})^2 + 6(\tau_{xy}^2 + \tau_{xz}^2 + \tau_{yz}^2) \right]^{1/2}. \quad (5.50)$$

⁸ K.L. Johnson, Contact mechanics. Cambridge University Press, Ninth printing 2003.

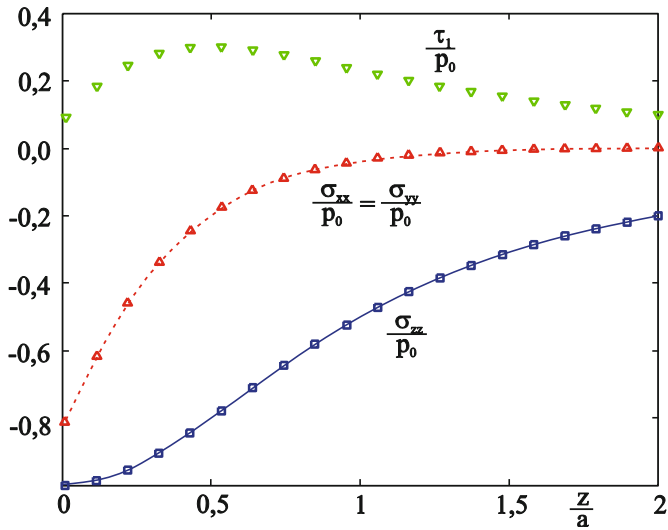


Fig. 5.8 Stresses along the z -axis ($x = y = 0$) for Hertzian pressure distribution.

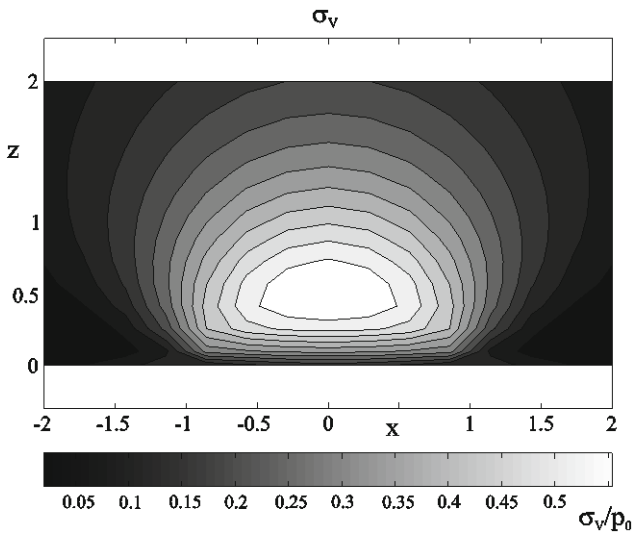


Fig. 5.9 Equivalent stress σ_v according to (5.50) for Hertzian pressure distribution (x - z plane).

5.6 Method of Dimensionality Reduction (MDR)

The contact of axial symmetric bodies with any shape can be easily and elegantly solved by the so-called Method of Dimensionality Reduction (MDR)⁹. The MDR maps a three-dimensional contact onto a contact with a one-dimensional array of independent springs (Winkler foundation), and it therefore simplifies both the analytical and the numerical treatment of the contact problem. Despite its simplicity, all results for axial-symmetric contacts are exact. With the MDR, non-adhesive and adhesive contacts, tangential contacts with friction, and contacts of viscoelastic media can be studied. In this section, we describe the application of the MDR for the treatment of normal contact problems. Generalizations for other problems will be discussed at appropriate sections in subsequent chapters. The proof of the correctness of the fundamental equations of the MDR is given in Appendix B.

The MDR basically consists of two simple steps: (a) replacement of the three-dimensional continuum by a strictly defined one-dimensional Winkler bedding and (b) transformation of the three-dimensional shape into a two-dimensional shape using the MDR-transformation. If these two steps are completed, the contact problem can be considered to be solved.

Two preliminary basic steps of the MDR

We consider a contact between two elastic bodies with moduli of elasticity of E_1 and E_2 and Poisson's numbers of ν_1 and ν_2 . We denote the difference between the profiles of the bodies as $z = f(r)$. In the framework of the MDR, two independent steps are conducted:

I. First, the three-dimensional elastic (or viscoelastic) bodies are replaced by a one-dimensional Winkler foundation. This is considered to be a linear array of elements having independent degrees of freedom and a sufficiently small separation distance Δx .

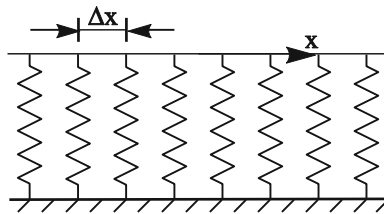


Fig. 5.10 One-dimensional elastic foundation.

⁹ V.L. Popov, M. Heß, Method of Dimensionality Reduction in Contact Mechanics and Friction, Springer, 2015.

In the simplest case of the elastic contact, the foundation consists of linearly elastic spring elements that have a normal stiffness Δk_z (Fig. 5.10):

$$\Delta k_z = E^* \Delta x, \tag{5.51}$$

where E^* is given by (5.26).

II. In the second step, the three-dimensional profile $z = f(r)$ (Fig. 5.11, left) is transformed into a one-dimensional profile (Fig. 5.11, right) according to

$$g(x) = |x| \int_0^{|x|} \frac{f'(r)}{\sqrt{x^2 - r^2}} dr \tag{5.52}$$

The reverse transformation is

$$f(r) = \frac{2}{\pi} \int_0^r \frac{g(x)}{\sqrt{r^2 - x^2}} dx. \tag{5.53}$$

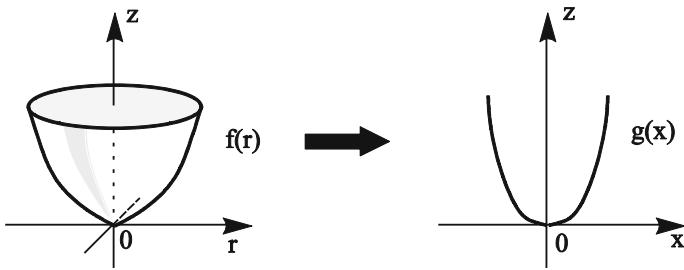


Fig. 5.11 The three-dimensional profile is transformed into a one-dimensional profile using the MDR

Calculation steps of the MDR

The one-dimensional profile according to (5.52) is now pressed into an elastic foundation corresponding to (5.51) with the normal force F_N (see Fig. 5.12).

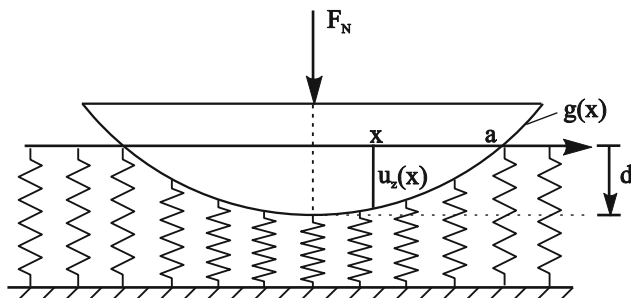


Fig. 5.12 Equivalent MDR model of normal contact.

The normal surface displacement at the point x within the contact area results from the difference between the indentation depth d and the profile form g :

$$u_z(x) = d - g(x). \quad (5.54)$$

At the edge of the non-adhesive contact $x = \pm a$, the surface displacement must be zero:

$$u_z(\pm a) = 0 \Rightarrow d = g(a). \quad (5.55)$$

This equation determines the relationship between the indentation depth and the contact radius a . It should be noted that this relationship is independent of the rheology of the medium. The force of a spring at the point x is proportional to the displacement at this point:

$$\Delta F_z(x) = \Delta k_z u_z(x) = E^* u_z(x) \Delta x. \quad (5.56)$$

The sum of all spring forces must correspond to the normal force in equilibrium. In the limiting case of very small spring separation distances $\Delta x \rightarrow dx$, the summation becomes the integral

$$F_N = E^* \int_{-a}^a u_z(x) dx = 2E^* \int_0^a (d - g(x)) dx. \quad (5.57)$$

Equation (5.57) provides the normal force with respect to the contact radius and the indentation depth if (5.55) is taken into account.

We now define the linear force density $q_z(x)$:

$$q_z(x) = \frac{\Delta F_z(x)}{\Delta x} = E^* u_z(x) = \begin{cases} E^* (d - g(x)), & |x| < a \\ 0, & |x| > a \end{cases}. \quad (5.58)$$

As shown in Appendix B, the stress distribution in the original three-dimensional system can be determined with the help of the one-dimensional force density using the integral transformation

$$p(r) = -\frac{1}{\pi} \int_r^\infty \frac{q'_z(x)}{\sqrt{x^2 - r^2}} dx. \quad (5.59)$$

The normal surface displacement $u_{3D,z}(r)$ (both inside and outside of the contact area) is given by the transformation:

$$u_{3D,z}(r) = \frac{2}{\pi} \int_0^r \frac{u_z(x)}{\sqrt{r^2 - x^2}} dx. \quad (5.60)$$

For the sake of completeness, we still give the reverse transformation to (5.59):

$$q(x) = 2 \int_x^{\infty} \frac{r p(r)}{\sqrt{r^2 - x^2}} dr. \quad (5.61)$$

Equations (5.52), (5.55), (5.57), (5.59), (5.60) solve the normal contact problem completely. In the problems of this chapter, several examples are discussed.

Problems

Problem 1: Estimate the maximum pressure and the size of the contact area in a rail-wheel contact. The maximum load per wheel is around $F \approx 10^5$ N for cargo trains, the wheel radius is ca. $R = 0.5$ m.

Solution: The rail-wheel contact can be regarded, in a first-order approximation, as the contact between two cylinders lying on axes perpendicular to each other with roughly the same radius R . Therefore, it is equivalent to the contact between an elastic sphere with the radius R and an elastic half-space. The effective modulus of elasticity is $E^* \approx E/2(1-\nu^2) \approx 1.2 \cdot 10^{11}$ Pa. The pressure in the center of the contact area is found to be $p_0 \approx 1.0$ GPa according to (5.24). The contact radius is $a \approx 6.8$ mm.

Problem 2: Two cylinders of the same material and with the same R are brought into contact so that their axes form an angle of $\pi/4$ (Fig. 5.13). Determine the relationship between force and penetration depth.

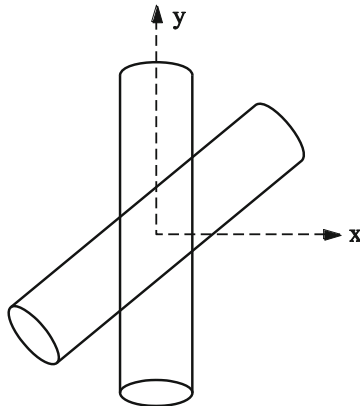


Fig. 5.13 Contact between two identical cylinders which form an angle of $\pi/4$ (when seen from above).

Solution: We assume that the contact plane is horizontal. The distance between the surface of the first cylinder and this plane (at the first moment of contact) is equal

to $z_1 = \frac{x^2}{2R}$, and the distance for the second cylinder is equal to $z_2 = -\frac{(x-y)^2}{4R}$.

The distance between both surfaces is then

$$h = \frac{x^2}{2R} + \frac{(x-y)^2}{4R} = \frac{1}{R} \left(\frac{3}{4}x^2 - \frac{1}{2}xy + \frac{1}{4}y^2 \right).$$

The principal curvatures are calculated as the eigenvalues of this quadratic form, using the equation,

$$\begin{vmatrix} \frac{3}{4R} - \kappa & -\frac{1}{4R} \\ -\frac{1}{4R} & \frac{1}{4R} - \kappa \end{vmatrix} = \kappa^2 - \frac{\kappa}{R} + \frac{1}{8R^2} = 0.$$

to $\kappa_{1,2} = \frac{1 \pm 1/\sqrt{2}}{2R}$. The principal radii of curvature are accordingly

$R_{1,2} = \frac{2R}{1 \pm 1/\sqrt{2}}$. The resulting Gaussian radius of curvature is

$\tilde{R} = \sqrt{R_1 R_2} = 2\sqrt{2}R$. Because both cylinders are made from the same material,

then according to (5.26) $E^* = \frac{E}{2(1-\nu^2)}$. In this case, the relationship between the

force and the penetration depth from (5.23) is

$$F = \frac{2^{7/4}}{3} \frac{E}{(1-\nu^2)} R^{1/2} d^{3/2}.$$

Problem 3: Determine the contact time during an impact of an elastic sphere (Radius R) with a flat wall (Hertz, 1882).

Solution: The displacement of the center of the sphere from the moment of initial contact we will call x . The potential energy of the system is given by (5.25) with $d = x$ and E^* according to (5.26). During the contact time, the energy is conserved:

$$\frac{m}{2} \left(\frac{dx}{dt} \right)^2 + \frac{8}{15} E^* R^{1/2} x^{5/2} = \frac{mv_0^2}{2}.$$

The maximum displacement x_0 corresponds to the point in time at which the velocity, dx/dt , is zero and is

$$x_0 = \left(\frac{15}{16} \frac{mv_0^2}{E^* R^{1/2}} \right)^{2/5}.$$

The contact time τ (during which x varies from 0 to x_0 and again back to 0) is

$$\tau = \frac{2}{v_0} \int_0^{x_0} \frac{dx}{\sqrt{1 - (x/x_0)^{5/2}}} = \frac{2x_0}{v_0} \int_0^1 \frac{d\xi}{\sqrt{1 - \xi^{5/2}}} = \frac{2,94x_0}{v_0}.$$

Problem 4: Determine the maximum contact pressure during an impact between a sphere and a wall.

Solution: We calculated the maximum indentation depth x_0 in Problem 3. The maximum pressure p_0 is given by (5.22) and is equal to

$$p_0 = \frac{2}{\pi} E^* \left(\frac{x_0}{R} \right)^{1/2} = \frac{2}{\pi} \left(\frac{15}{16} \frac{E^{*4} mv_0^2}{R^3} \right)^{1/5} = \frac{2}{\pi} \left(\frac{5}{4} \pi E^{*4} \rho v_0^2 \right)^{1/5},$$

where ρ is the density of the material.

For example, by the impact of a steel sphere on a steel wall at $v_0 = 1$ m/s, we have (assuming a purely elastic collision)

$$p_0 \approx \frac{2}{\pi} \left(\frac{5}{4} \pi (10^{11})^4 (7.8 \cdot 10^3) \cdot 1 \right)^{1/5} = 3.2 \cdot 10^9 \text{ Pa}.$$

Problem 5: Determine the differential contact stiffness $\delta F_N / \delta d$ for a contact between an elastic axially symmetric body and a rigid plane with a contact area A (Fig. 5.14).

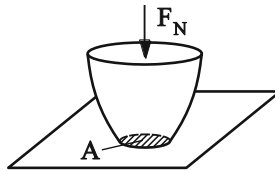


Fig. 5.14 Contact between an elastic, axially-symmetric body and a rigid plane.

Solution: We consider a round contact area with a radius a . The change in the area of the contact due to the infinitesimally small increase of the penetration depth δd can be thought of as taking place in two steps:

First, the existing contact area is rigidly displaced by δd (Fig. 5.15 b). Thereby, the normal force changes according to (5.12) by $\delta F_N = 2aE^* \delta d$. In the second step, the remaining raised boundary area must then be displaced the same distance (Fig. 5.15 c). The increase in the given normal force is thereby proportional to the

area $2\pi a\delta a$ and to the height of the remaining raised boundary area. Therefore, the infinitesimally small change in force for the second step is of a higher order and can be neglected. The differential stiffness,

$$k_z = \frac{\delta F_N}{\delta d} = 2aE^*,$$

is, therefore, only dependent on the contact radius and not on the exact form of the axially-symmetric body. For non-axially symmetric bodies, equation (5.13) is valid for the differential stiffness.

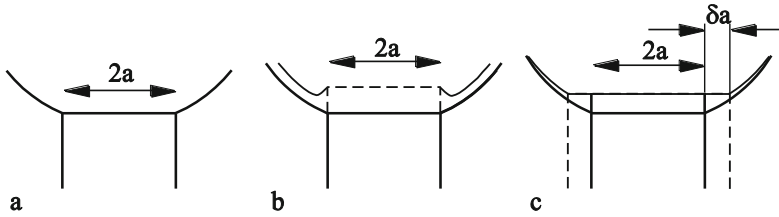


Fig. 5.15 Calculating the differential stiffness.

Problem 6: A constant distributed stress, p_0 , acts on a circular contact area with a radius a . Determine the displacement at the center and the boundary of the circular area.

Solution: With help from (5.7) we obtain the following for the displacement in the center of the circle:

$$u_z(0) = \frac{1}{\pi E^*} \int_0^a p_0 \frac{2\pi r}{r} dr = \frac{2p_0 a}{E^*}.$$

The displacement at the boundary is

$$u_z(a) = \frac{1}{\pi E^*} \int_0^{2a} p_0 \frac{2\varphi(r) \cdot r}{r} dr = \frac{p_0}{\pi E^*} \int_0^{2a} 2\varphi(r) dr.$$

(See Fig. 5.16 for the definition of the integration variable r in this case). The angle φ is calculated as $2\varphi = \pi - 2 \arcsin\left(\frac{r}{2a}\right)$. Therefore, we obtain

$$u_z(a) = \frac{p_0}{\pi E^*} \int_0^{2a} \left(\pi - 2 \arcsin\left(\frac{r}{2a}\right) \right) dr = \frac{2ap_0}{\pi E^*} \int_0^1 \left(\pi - 2 \arcsin(\xi) \right) d\xi = \frac{4ap_0}{\pi E^*}.$$

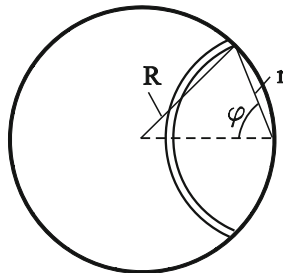


Fig. 5.16 Calculation of the integral in Problem 6.

Problem 7: Use the Method of Dimensionality Reduction to solve the normal contact problems between an elastic half-space and a rigid indenter with the following profiles:

- (a) flat cylindrical indenter with radius a : $f(r) = \begin{cases} 0, & r < a \\ \infty, & r \geq a \end{cases}$,
- (b) parabolic profile $f(r) = r^2 / (2R)$,
- (c) conical profile $f(r) = r \cdot \tan \theta$,
- (d) power function profile $f(r) = c_n r^n$ with arbitrary power n .

Solution: In order to use the MDR, the equivalent profile must first be calculated by means of the transformation (5.52). A simple calculation for the profiles listed above follows:

- (a) $g(x) = \begin{cases} 0, & |x| < a \\ \infty, & |x| \geq a \end{cases}$,
- (b) $g(x) = x^2 / R$,
- (c) $g(x) = \frac{\pi}{2} |x| \tan \theta$,
- (d) $g(x) = \kappa_n c_n |x|^n$

with $\kappa_n = \frac{\sqrt{\pi}}{2} \frac{n\Gamma(\frac{n}{2})}{\Gamma(\frac{n}{2} + \frac{1}{2})}$, where $\Gamma(n) = \int_0^\infty t^{n-1} e^{-t} dt$ is the Gamma-function.

The contact radius is given by $g(a) = d$, (5.55):

- (a) contact radius is constant and equal to a ,
- (b) $a = \sqrt{Rd}$,
- (c) $a = \frac{2}{\pi} \frac{d}{\tan \theta}$,
- (d) $a = \left(\frac{d}{\kappa_n c_n} \right)^{1/n}$.

The normal force for the given indentation depth is calculated according to (5.57):

$$\begin{aligned} \text{(a)} \quad F_N &= 2E^* ad, \\ \text{(b)} \quad F_N &= \frac{4}{3} E^* R^{1/2} d^{3/2}, \\ \text{(c)} \quad F_N &= \frac{2}{\pi} E^* \frac{d^2}{\tan \theta}, \\ \text{(d)} \quad F_N &= \frac{2nE^*}{n+1} (\kappa_n c_n)^{\frac{1}{n}} d^{\frac{n+1}{n}}. \end{aligned}$$

In order to calculate the pressure distribution in the three-dimensional original problem, the linear load should first be calculated according to the definition (5.58) in the MDR:

$$\begin{aligned} \text{(a)} \quad q_z(x) &= \begin{cases} E^* d, & |x| < a \\ 0, & |x| > a \end{cases}, \\ \text{(b)} \quad q_z(x) &= \begin{cases} E^* (d - x^2 / R), & |x| < a \\ 0, & |x| > a \end{cases}, \\ \text{(c)} \quad q_z(x) &= \begin{cases} E^* \left(d - \frac{\pi}{2} |x| \tan \theta \right), & |x| < a \\ 0, & |x| > a \end{cases}, \\ \text{(d)} \quad q_z(x) &= \begin{cases} E^* (d - \kappa_n c_n |x|^n), & |x| < a \\ 0, & |x| > a \end{cases}. \end{aligned}$$

The derivation of the linear load at x (for a positive x) is calculated as

$$\begin{aligned} \text{(a)} \quad q_z'(x) &= -E^* d \cdot \delta(x-a), \text{ where } \delta(x) \text{ is the Dirac delta function,} \\ \text{(b)} \quad q_z'(x) &= \begin{cases} -2E^* x / R, & x < a \\ 0, & x > a \end{cases}, \\ \text{(c)} \quad q_z'(x) &= \begin{cases} -\frac{\pi}{2} E^* \tan \theta, & x < a \\ 0, & x > a \end{cases}, \\ \text{(d)} \quad q_z'(x) &= \begin{cases} -E^* \kappa_n c_n n x^{n-1}, & x < a \\ 0, & x > a \end{cases}. \end{aligned}$$

Substituting the derivative into (5.59) the pressure distribution in the contact area is obtained:

$$\text{(a)} \quad p(r) = \frac{E^* d}{\pi} \int_r^\infty \frac{\delta(x-a)}{\sqrt{x^2 - r^2}} dx = \begin{cases} \frac{E^* d}{\pi} \frac{1}{\sqrt{a^2 - r^2}}, & r < a \\ 0, & r > a \end{cases},$$

(b)

$$p(r) = \frac{2E^*}{\pi R} \int_r^\infty \frac{x}{\sqrt{x^2 - r^2}} dx = \begin{cases} \frac{2E^*}{\pi R} \int_r^a \frac{x}{\sqrt{x^2 - r^2}} dx = \frac{2E^*}{\pi R} \sqrt{a^2 - r^2}, & r < a \\ 0, & r > a \end{cases},$$

(c)

$$p(r) = \frac{E^*}{2} \tan \theta \int_r^\infty \frac{dx}{\sqrt{x^2 - r^2}} = \frac{E^*}{2} \tan \theta \int_r^a \frac{dx}{\sqrt{x^2 - r^2}} = \frac{E^*}{2} \tan \theta \cdot \ln \left(\frac{a}{r} + \sqrt{\left(\frac{a}{r}\right)^2 - 1} \right)$$

for $r < a$ and $p(r) = 0$ outside the contact area,

$$(d) \quad p(r) = \kappa_n c_n n \frac{E^*}{\pi} \int_r^\infty \frac{x^{n-1}}{\sqrt{x^2 - r^2}} dx = \begin{cases} \kappa_n c_n n \frac{E^*}{\pi} \int_r^a \frac{x^{n-1}}{\sqrt{x^2 - r^2}} dx, & r < a \\ 0, & r > a \end{cases}.$$

If we normalize the pressure with the mean pressure in the contact region $\bar{p} = F_N / (\pi a^2)$ and the polar radius with the contact radius $\tilde{r} = r / a$, we can write the pressure in the contact area in the form

$$\frac{p(r)}{\bar{p}} = \frac{n+1}{2} \int_{\tilde{r}}^1 \frac{\xi^{n-1}}{\sqrt{\xi^2 - \tilde{r}^2}} d\xi.$$

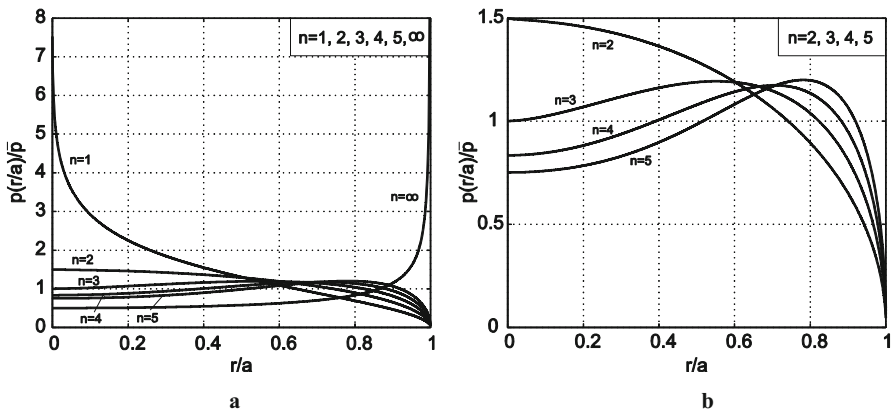


Fig. 5.17 Pressure distribution for simple power function profile (a) for $n = 1, 2, 3, 4, 5, \infty$, (b) a detail with higher resolution for $n = 2, 3, 4, 5$.

Although this integral can be represented for all integers n via elementary functions, it is easier to calculate it numerically. The pressure distributions for $n = 1$ (cone), $n = 2$ (Hertzian contact), $n = 3$, $n = 4$, $n = 5$ and $n = \infty$ (flat cylindrical punch) are shown in Fig. 5.17 for comparison. For the cone, the pressure has a logarithmic singularity at the tip of the cone. The pressure distribution for all cases with $n > 1$ is not singular, but the maximum pressure for $n = 2$ appears in the cen-

ter of the contact. Then, for larger n it begins to move towards the edge of the contact area. In the limiting case $n = \infty$, which corresponds to a flat cylindrical punch, the pressure distribution is singular at the edge of the contact area.

Normal displacements outside the contact area ($r > a$) are given by (5.60). The explicit form is

$$u_{3D,z}(r) = \frac{2}{\pi} \int_0^a \frac{u_z(x)}{\sqrt{r^2 - x^2}} dx = \frac{2}{\pi} \int_0^a \frac{d - g(x)}{\sqrt{r^2 - x^2}} dx, \quad \text{for } r > a.$$

For these special cases (a)-(d) we have:

- (a) $u_{3D,z}(r) = \frac{2d}{\pi} \arcsin\left(\frac{a}{r}\right),$
- (b) $u_{3D,z}(r) = \frac{d}{\pi} \left[\left(2 - \left(\frac{r}{a}\right)^2 \right) \cdot \arcsin\left(\frac{a}{r}\right) + \sqrt{\left(\frac{r}{a}\right)^2 - 1} \right],$
- (c) $u_{3D,z}(r) = \frac{2d}{\pi} \left[\arcsin\left(\frac{a}{r}\right) - \left(\frac{r}{a} - \sqrt{\left(\frac{r}{a}\right)^2 - 1} \right) \right],$
- (d) $u_{3D,z}(r) = \kappa_n c_n \frac{2}{\pi} \int_0^a \frac{a^n - x^n}{\sqrt{r^2 - x^2}} dx.$

In case (d), we did not carry out an explicit integration.

Problem 8: With the method of dimensionality reduction, determine the relations between normal force, indentation depth, and contact radius of a flattened parabolic profile (Fig. 5.18):

$$f(r) = \begin{cases} 0 & \text{for } 0 \leq r < b \\ \frac{r^2 - b^2}{2R} & \text{for } b \leq r \leq a \end{cases}$$

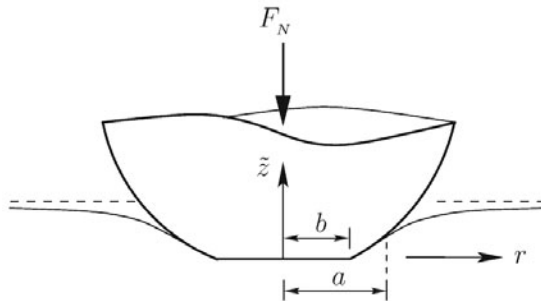


Fig. 5.18 Qualitative illustration of a flattened parabolic profile pressed into an elastic half-space.

Solution: To calculate the MDR-transformed profile according to (5.52), we first calculate the derivative of the original profile:

$$f'(r) = \begin{cases} 0 & \text{for } 0 \leq r < b \\ \frac{r}{R} & \text{for } b \leq r \leq a \end{cases} .$$

Substituting it into (5.52) and subsequently integrating it gives

$$g(x) = \begin{cases} 0 & \text{for } 0 \leq |x| < b \\ \frac{|x|}{R} \sqrt{x^2 - b^2} & \text{for } b \leq |x| \leq a \end{cases} .$$

This profile is shown in Fig. 5.19 as compared to the original.

The indentation depth as a function of the contact radius is obtained from (5.55)

$$d = g(a) = \frac{a}{R} \sqrt{a^2 - b^2} .$$

The normal force is obtained as the sum of all spring forces

$$F_N = E^* \int_{-a}^a [d - g(x)] dx = 2E^* \int_0^a d dx - \frac{2E^*}{R} \int_b^a x \sqrt{x^2 - b^2} dx ,$$

which provides the following result after integration and appropriate transformations:

$$F_N(a) = \frac{2E^*}{3R} (2a^2 + b^2) \cdot \sqrt{a^2 - b^2} .$$

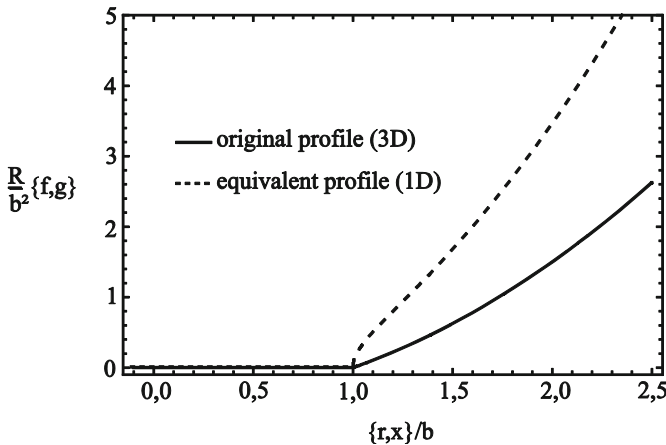


Fig. 5.19 Parabolic indenter with a worn tip: its original and equivalent profile.

For the sake of completeness, the relationship between normal force and indentation depth is given here:

$$F_N(d) = \frac{\sqrt{2}E^*b^3}{3R} \left(2 + \sqrt{1 + \left(\frac{2R}{b^2} d \right)^2} \right) \cdot \sqrt{-1 + \sqrt{1 + \left(\frac{2R}{b^2} d \right)^2}} .$$